Label-Free Electrical Detection of DNA Hybridization on Graphene using Hall Effect Measurements: Revisiting the Sensing Mechanism

Cheng-Te Lin, Phan Thi Kim Loan, Tzu-Yin Chen, Keng-Ku Liu, Chang-Hsiao Chen, Kung-Hwa Wei, and Lain-Jong Li**

There is broad interest in using graphene or graphene oxide sheets as a transducer for label-free and selective electrical detection of biomolecules such as DNA. However, it is still not well explored how the DNA molecules interact with and influence the properties of graphene during the detection. Here, Hall effect measurements based on the Van der Pauw method are used to perform single-base sequence selective detection of DNA on graphene sheets, which are prepared by chemical vapor deposition. The sheet resistance increases and the mobility decreases with the addition of either complementary or one-base mismatched DNA to the graphene device. The hole carrier concentration of the graphene devices increases significantly with the addition of complementary DNA but it is less affected by the one-base mismatched DNA. It is concluded that the increase in hole carrier density, indicating p-doping to graphene, is better correlated with the DNA hybridization compared to the commonly used parameters such as conductivity change. The different electrical observations of p-doping from Hall effect measurements and n-doping from electrolyte-gated transistors can be explained by the characteristic morphology of partially hybridized DNA on graphene and the mismatch between DNA chain length and Debye length in electrolytes.

1. Introduction

Interfacing bio-objects with nanomaterials is becoming one of the most diverse and dynamic areas of science and technology. The research of nano/bio interfaces, such as the interaction between biomolecules and nanomaterial surfaces, is rapidly growing.[1] Carbon nanotubes are highly sensitive to environmental perturbations; therefore, they have been widely used for sensors based on electrochemical, optical, or electrical transductions.[2–6] Among these approaches, label-free electrical detection has attracted extensive research efforts because no fluorescent or electrochemical tags are required.[7–10] In addition to the carbon nanotubes, graphene with a 2D structure has been emerging as one of the building blocks for nanoelectronic biosensors due to its high carrier mobility[11] and low intrinsic electrical noises.[12] Moreover, the conductance of graphene sheet is highly sensitive to the local perturbations from chemicals or charges, and its two-dimensionality makes it suitable to interface with flat cell membranes. Graphene derivatives, such as graphene oxide (GO) and reduced graphene oxide (rGO), have also been extensively studied.[13–16] A number of sensing applications has been demonstrated using GO or rGO,[17] such as detection of chemicals,[18–21] proteins,[22] DNA hybridizations,[23–25] and cellular activities.[26] The label free electrical detection of DNA hybridization using bottom-gated devices produced from GO or rGO has been reported recently, where the DNA molecules are found to act as potential gating agents that impose p-doping[27] in graphene layers. Note that the transfer curves of these sensor devices exhibit a low on/off current ratio (or resistor-like behavior); hence, the detection was mainly based on the device conductivity change.[25,27] Since the conductivity of graphene materials is very sensitive to the scattering process from the Coulomb charges including the DNA molecules and the ions in buffer solution,[28] unambiguous detection of DNA hybridization based on the conductivity change may require more specific measurement conditions to demonstrate reasonable reproducibility. Meanwhile, it is speculated that the interaction between rGO and DNA molecules strongly depends on the size or defect content of the rGO sheets, which in turns affects the detection performance.[27] The recent success in obtaining large-area graphene films by chemical vapor deposition (CVD) methods likely make graphene-based biosensors practical[29–31] because the top-down microlithography fabrication of biosensor devices is possible for CVD graphene films. For instance a label-free electrical detection of DNA hybridization using electrolyte-gated field-effect transistor (FET) configuration based on few-layered CVD graphene films has been

Dr. C.-T. Lin, T.-Y. Chen, K.-K. Liu, C.-H. Chen, Prof. L.-J. Li
Institute of Atomic and Molecular Sciences
Academia Sinica, Taipei, 10617, Taiwan
E-mail: lanceli@gate.sinica.edu.tw
P. T. K. Loan, K.-H. Wei
Department of Material Science and Engineering
National Chiao Tung University
Hsinchu 300, Taiwan
E-mail: khwei@mail.nctu.edu.tw

DOI: 10.1002/adfm.201202672

reported,[32,33] where the negative shift of the neutrality point voltage (valley point of the ambipolar transfer curve; V_{CNP}) is correlated to the DNA hybridization event. The left shift was ascribed to the n-doping of graphene from the nucleosides of DNA.[25,27] However, some other studies have indicated that the attachment of a single-stranded DNA (ssDNA) on graphene results in an increase of hole carrier concentration (p-doping of graphene).[27,34] The controversial explanations may arise from the fact that the transport characteristics of graphene observed with electrolyte gating are strongly related to graphene/solution interface properties, which are complicated by the adsorption of DNA and counter ions on graphene, the screening of DNA charges by counter ions, as well as the morphology of single-stranded and hybridized DNA.

In this contribution, we fabricate the devices based on CVD graphene films for the electrical detection of DNA hybridization, where the Hall effect measurement[35] and solution gating experiment can be performed in the same device platform. The effects on hole carrier concentration, sheet resistance, and hole carrier mobility for DNA adsorption and hybridization on graphene devices are systematically studied. Surprisingly, the sheet resistance (hole carrier mobility) does not exclusively increase (decrease) with the addition of complementary DNA; these two parameters also apparently change with the addition of one-base mismatched DNA. However, the hole carrier concentration (density) increase is well related to the addition of complementary DNA, not one-base mismatched DNA, suggesting that the Hall effect measurement involving graphene is likely a more reliable detection method for DNA hybridization than the ones based on the conductivity or mobility change. This work also provides possible explanations for the different observations in the Hall effect and electrolyte gating measurements.

2. Results and Discussion

Graphene monolayers were grown on Cu foils by CVD as reported previously by several groups.[36,37] As grown graphene on Cu was spin-coated with a support layer of poly(methyl methacrylate) (PMMA),[30] and the PMMA/graphene/copper film was soaked in a ferric nitrate solution at 60 °C for several hours to etch the copper foil. The PMMA protected graphene layer was temporarily supported by a glass slide and washed with deionized (DI) water and hydrochloric acid to remove metal ions. After cleaning, the PMMA-protected graphene layers were suspended in DI water again. A 300 nm SiO_2/Si substrate was used to fish the film. For removal of PMMA, The sample was immersed in acetone at 55 °C to dissolve PMMA, and then annealed at 450 °C in H_2/Ar. Electrodes were made by applying silver paste at the four corners of the graphene sheets (5 mm × 5 mm) to form a four-point contacted device for Hall effect measurements. For the electrolyte gating experiment, silicone rubber (Dow Corning 3140) was spread surrounding the edges of graphene to create a reservoir for hosting solution analytes. These four electrodes were also protected by rubber for the insulation from electrolytes as schematically illustrated in **Figure 1**a. Two of these electrodes are used as source and drain contacts and a silver wire is used as the gate to realize a liquid-gated FET, where the top view of the device built on a sample holder is shown in Figure 1b. Figure 1c shows the set up of the Hall effect measurement based on the Van der Pauw method, where a permanent magnet is used to provide a magnetic field. The sample shown in Figure 1b can be positioned at the center of the magnet. The 12-mer sequences of the probe, complementary, and one-base mismatched DNA are shown in Figure 1a.

The procedures to add in the probe, complementary and mismatched DNA are similar to our previous report.[32] In brief, before the addition of probe DNA molecules, the pure phosphate buffered saline (PBS) solution (40 μL) was added in the reservoir as an electrolyte for obtaining the transfer curve (drain current vs gate voltage) of the pristine graphene. After removing the pure PBS buffer solution, the probe DNA (10 μM in 40 μL PBS buffer) were then added in for 16 h for allowing their attachment to the graphene surfaces by physical adsorption. The graphene was then rinsed with PBS solution to remove the weakly-bound DNA molecules. Hybridization was performed by adding 40 μL of complementary or one-base mismatched DNA to the probe DNA-immobilized graphene device for 4 h, followed by water rinsing and drying. The pure PBS (40 μL) was added again in the reservoir as the electrolyte for measuring the transfer curves. Inset of **Figure 2**a shows the transfer curves for graphene FET device before and after each DNA addition step. The immobilization of probe DNA (10 μM) onto the pristine graphene does not necessarily cause a consistent left- of right-shift in V_{CNP}, although the specific sample discussed in Figure 2a shows a slight left-shift (from 0.45 V to 0.44 V after addition of probe DNA). Supporting Information Figure S1 shows the electrical results for another two graphene samples, respectively, presenting the left- and right-shift in V_{CNP} after probe DNA immobilization. However, the hybridization reaction (by addition of complementary DNA) always causes a left-shift in V_{CNP}. Note that the negative shift of the threshold voltage of carbon nanotube transistors after DNA immobilization has been attributed to the electron transfer from electron-rich aromatic nucleotide bases in DNA.[38,39] The electron transfer (n-doping) from DNA to graphene may occur similarly.[25,32] In contrast to the n-doping model, several recent studies have indicated that molecular gating from the negatively charged ions increases the hole carrier concentration in graphene, i.e., p-doping, based on the observation that the conductivity increases with the extent of DNA immobilization[22,27,34] or hybridization[27] on graphene. To properly characterize the change of carrier properties in graphene, a direct measurement based on the Hall effect measurement during the sensing process is performed. The polarity of the carriers in graphene is determined to be dominated by positive charges (holes), which is consistent with the common belief that graphene is p-doped in ambient. Figure 2b shows that the obtained hole carrier concentration of graphene increases unambiguously with the concentration increase of attached complementary DNA, either measured in "dry" (without PBS) or "wet" (in PBS) states. This trend agrees with the p-doping speculation. New insights are therefore needed to explain the inconsistency between the left-shift of V_{CNP} (Figure 2a) and the increase of the hole concentration (Figure 2b). Note that the "wet" state refers to the measurement when the graphene is covered with PBS solution, where

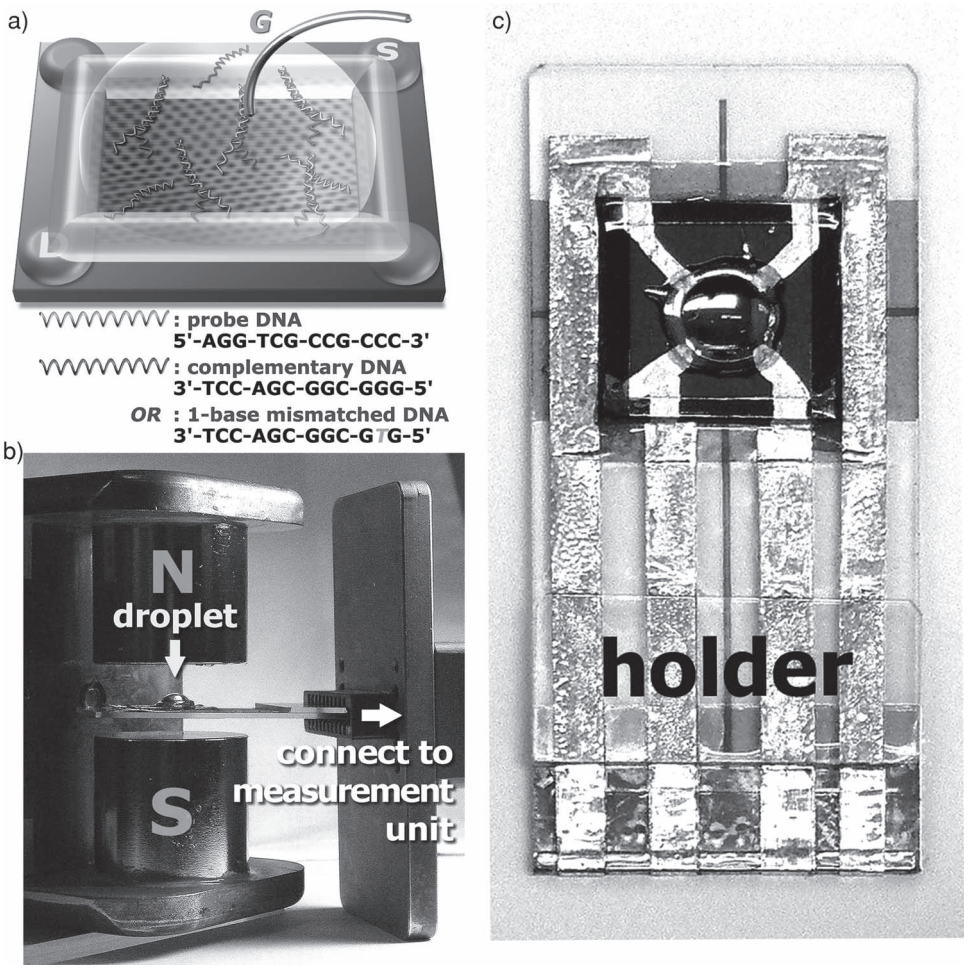

Figure 1. a) Schematic illustration of the graphene device designed for Hall effect and electrolyte gating experiments. Two of these electrodes are used as source and drain contacts and a silver wire is used as the gate for FET measurements. b) Top view of the device built on a sample holder. c) The setup of the Hall effect measurement based on the Van der Pauw method, where a permanent magnet is used to provide a magnetic field.

no gate metal is inserted. Hence, the hole carrier density of the "dry" state does not vary much with that of the "wet" state. It is commonly believed that there exists an adsorbed moisture layer on graphene when the graphene is left in air. Therefore, in our Hall effect measurement, the difference between "dry" and "wet" states is not very significant.

Figure 3a–c shows the hole carrier concentration, hole carrier mobility and sheet resistance for two graphene devices subjected to the addition of complementary and one-base mismatched DNA, respectively. The graphene devices were immobilized with probe DNA before the addition of complementary or one-base mismatched DNA. These measurements done in dry and PBS solution, respectively, show a similar trend. According to Van der Pauw theory, the hole carrier concentration (n) and sheet resistance (R) are directly determined by the measurements. And the hole mobility (μ) can be evaluated by the equation: $\mu \propto 1/Rn$. After we carefully analyze our results (e.g., in PBS), we observe that in Figure 3a the hole carrier concentration of graphene devices (red solid line) increases significantly with the concentration of added complementary DNA. In contrast, the hole carrier concentration of the devices (blue dot line) is not affected appreciably by the concentration of the added one-base mismatched DNA. And the sheet resistance increase (Figure 3b) caused by complementary DNA (+11.2%) is smaller than that by one-base mismatched DNA (+21.1%). Therefore, the hole mobility (Figure 3c) drop caused by the complementary DNA (–25.4%) becomes larger than that by one-base mismatched DNA (–18.8%). Measurements for more devices (shown in Supporting Information Table S1) enable us to conclude the generality of the observations. From the above arguments, the sheet resistance increases and the mobility decreases with the concentration of added either complementary or one-base mismatched DNA for graphene-based devices. However, the hole carrier concentration increases significantly after the addition of complementary DNA but not for the case of one-base mismatched DNA. This indicates that the change of sheet resistance or mobility may not be as selective as the carrier concentration for DNA hybridization. Therefore, the determination of carrier density is a more sensible detection method to differentiate the complementary and mismatched

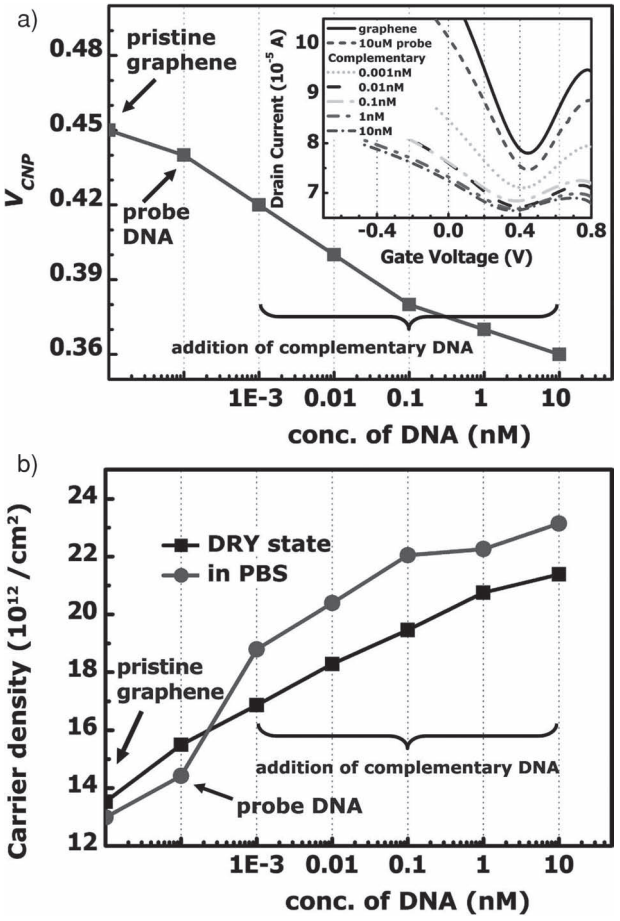

Figure 2. a) The V_{CNP} as a function of the concentration of added complementary DNA, where the V_{CNP} of the pristine and probe DNA-immobilized graphene is also included. Inset shows the transfer curves for the graphene devices before and after each DNA addition step. b) The carrier concentration of graphene as a function of the concentration of added complementary DNA. Two curves were measured separately in dry (without PBS) and wet (in PBS) states.

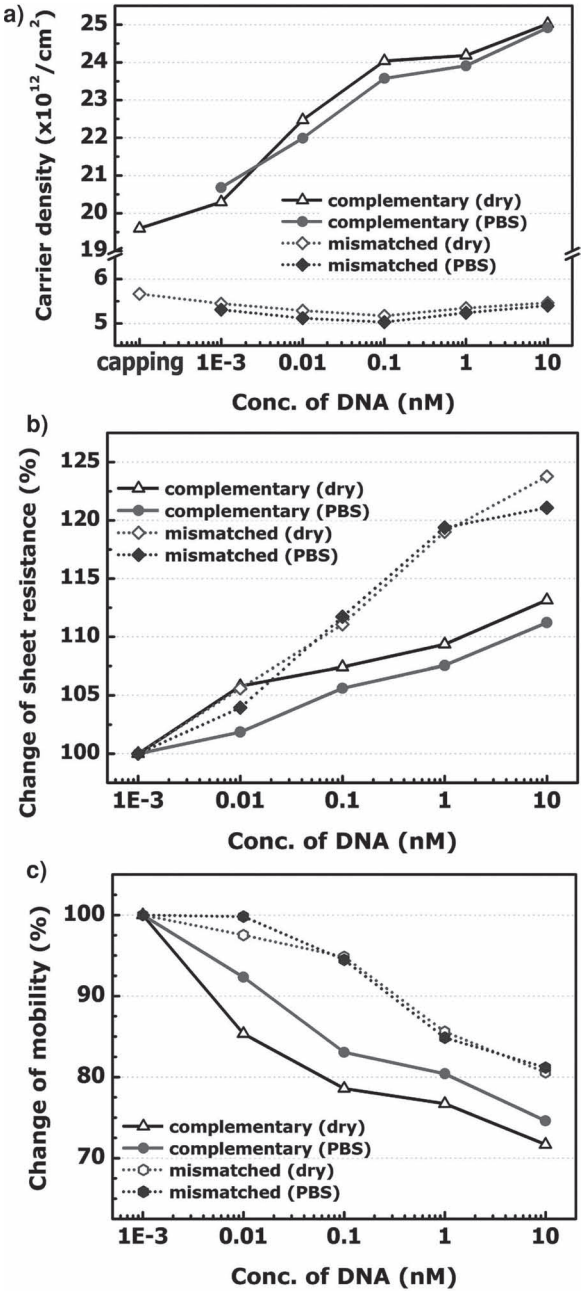

Figure 3. a) The hole carrier concentration, b) sheet resistance, and c) hole carrier mobility for the two probe DNA-immobilized graphene devices separately subjected to the addition of complementary and one-base mismatched DNA from 10^{-3} (1 pM) to 10 nM. These electrical characteristics were determined by the Hall effect measurement.

DNA. As shown in Supporting Information Figure S2, the statistical results obtained from the measurement of six devices demonstrate that the increased hole carrier density is positively correlated to the concentration of the complementary DNA. Note that the change of hole carrier density for the case of non-complementary DNA is also not obvious (see Supporting Information Figure S3). Two other different pairs of 22-mer probe/1-base mismatched DNA were also examined and the results are consistent (see Supporting Information Table S2).

To understand the interaction between DNA and graphene surfaces, several control experiments are performed. **Figure 4**a shows that the V_{CNP} shifts to the left when the graphene device is immobilized with the nucleoside guanosine. Supporting Information Figure S4 shows that other nucleosides also induce a left-shift in V_{CNP}. All the nucleosides similarly reduce the hole carrier concentrations based on the Hall effect measurements (see Supporting Information Table S3), indicating that the nucleosides impose n-doping to graphene sheets. On the other hand, Figure 4b shows that the V_{CNP} shifts to the right when the graphene device is immobilized with a double-stranded DNA (dsDNA). The dsDNA is fully hybridized by mixing the same molar number of probe and complementary DNA before adding onto graphene surfaces, where most of the DNA nucleosides are bonded to their complementary ones and some nucleosides may directly contact with graphene surfaces, as illustrated in Figure 4c. The hole carrier concentration of graphene increases

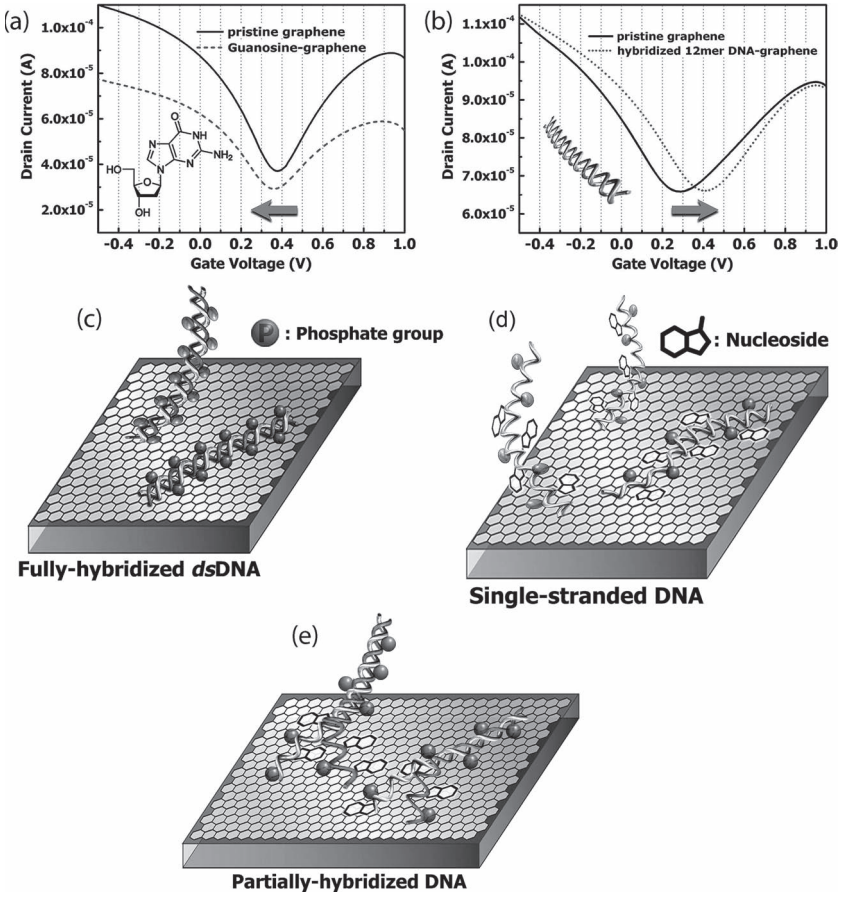

Figure 4. The transfer curves for a graphene device before and after interacting with a) the guanosine nucleoside and b) a dsDNA hybridized from the probe and complementary DNA. Schematic illustration for the interaction between graphene and c) fully hybridized dsDNA, d) ssDNA, and e) partially hybridized DNA.

after the addition of dsDNA. Note that the isoelectric point of DNA is pH ≈ 5.0[40,41] and DNA molecules should be negatively charged due to the phosphate groups when pH value is above 5.0. Hence, dsDNA should be negatively charged in 1× PBS (pH ≈ 7.9), where the charges adjacent to the graphene surfaces can induce an increase in the number of hole carriers in graphene. In electrolyte gating, more positive gate voltage is needed to screen off these negative charges at graphene surfaces to reach the V_{CNP}; thus, a positive shift of V_{CNP} is expected (Figure 4b). As revealed in Supporting Information Figure S5a, we have verified that the positive V_{CNP} shift and the increase of the hole carrier concentration are also observed for a longer dsDNA, which is formed from one 60-mer probe and one 60-mer complementary DNA sequences. Note that the V_{CNP} shift or carrier concentration change may become random (positive or negative) if the sequence of 60-mer ssDNA can form a hairpin loop structure (see Supporting Information Figure S5b,c and Table S4 for details). Since those DNA strands with self-assembling hairpin loops form cannot well-hybridize with each other, the electrical results would depend on the morphology of ssDNA adsorbed on graphene surfaces. The characteristic is similar to the short-chain ssDNA, as discussed below.

In a typical DNA sensing experiment, a 12-mer *ss*DNA (probes) is first added and lies on graphene surfaces, and the graphene is affected by the competing interaction from the nucleosides and the phosphate groups, as schematically illustrated in Figure 4d; hence, the direction of V_{CNP} shift likely varies with the morphology of the ssDNA adsorbed on graphene surfaces (see Supporting Information Table S5). The control experiments using long-chain ssDNA molecules (60-mer) also show the same phenomenon (see Supporting Information Table S6). Once the complementary DNA is added, however, the hybridized DNA strands become rigid and stand up on the graphene surfaces.[42] Since the electrolyte gating experiment still reveals a left-shift in V_{CNP}, we suspect that some of the nucleosides from the probe DNA segments are still strongly adhered to the graphene surfaces, and the hybridized DNA segments are standing up in PBS solution as depicted in Figure 4e. If we consider the fact that Debye length of the electrolyte (1× PBS) is ≈0.76 nm, and our DNA sequence composed of 12 bases is approximately 4 nm in length,[27,43] most of the negative charges should lie outside the Debye length. It is likely that the nucleosides adhered to graphene play a key role in the left-shift of V_{CNP}. However, the hole carrier concentration is dominated by the negative charges adjacent to graphene surfaces, where the negative phosphate ions of the hybridized DNA segments can still contribute to the overall hole carrier concentration. **Table 1** summarizes the general observations for V_{CNP} shift and hole carrier concentration change for graphene devices with different treatments, including immobilizations with nucleosides, dsDNA, ssDNA, and DNA hybridization. This report may stimulate further

Table 1. The change of electrical characteristics of graphene after interacting with nucleosides and various DNA structures.

	Nucleosides	Double-Stranded DNA	Single-Stranded DNA[b)]	DNA Hybridization (partially hybridized DNA)
Shift of V_{CNP} (electrolyte gating)	left	right	left (most cases)	left
Hole carrier concentration[a)]	decrease	increase	increase (most cases)	increase

[a)]Determined by Hall effect measurements; [b)]See Supporting Information Table S5 for details.

understanding of the surface interaction between graphene and biomolecules, and studies on graphene-based biosensors.[44–46]

3. Conclusions

We have constructed liquid-gated FETs based on single-layer CVD graphene with the detection limit of 1 pM (10^{-12} M) for DNA hybridization.[47] However, the interaction between DNA and graphene surfaces could not be clearly understood by only examining the FET results. Using the Hall effect measurement based on Van der Pauw method, we conclude that the sheet resistance increases and the hole carrier mobility decreases with the concentration of added either complementary or one-base mismatched DNA for graphene-based devices. Whereas, the hole carrier density of graphene devices increases significantly with the concentration of added complementary DNA but is not affected appreciably by the concentration of added one-base mismatched DNA. This indicates that the determination of the hole carrier concentration using graphene devices is a more sensible single base-specific detection method than the conductivity or mobility sensing techniques. The differentiation between complementary and one-base mismatched DNA can achieve high sensitivity at least as low as 10 pM (10^{-11} M). In addition, p-doping of graphene by DNA hybridization is observed in Hall effect measurements, but the charge neutral point shifts to left (indicating n-doping) in a liquid-gated configuration using the same device. Such an observation can be explained by the characteristic morphology of partially hybridized-DNA on graphene, and the mismatch between DNA chain length and Debye length in electrolytes.

4. Experimental Section

CVD Synthesis and Transfer of Graphene: Large-area graphene films were synthesized on copper foil (Alfa Aesar, item No.13382, purity: 99.8%) with 25 μm thickness by CVD. Prior to growth, the copper foil was heated in hydrogen from room temperature to 1030 °C during 30 min, and then kept at 1030 °C for 60 min. While the gas mixture (CH_4: H_2 = 60: 15 sccm) was introduced into the system at 1030 °C, graphene layer was then formed on the surface of copper. After reaction for 20 min, the furnace was naturally cooled down. To transfer graphene onto 300 nm SiO_2/Si substrates, the graphene/copper films were spin-coated with a thin layer of PMMA. The PMMA (MicroChem Co. NANO PMMA 950 K A4) was utilized as a protective layer, followed by baking at 100 °C for 2 min. The PMMA/graphene/copper films were immersed in a ferric nitrate solution (0.05 g mL^{-1}, J. T. Baker ACS reagent 98%) at 60 °C for 6–8 h to dissolve the copper foil. The PMMA-supported graphene was washed in DI water and 1 N hydrochloric acid (Riedel-de Haën 37%) for 20 min. A 300 nm SiO_2/Si substrate was used to fish the PMMA/graphene layers, and PMMA was then dissolved in acetone (J. T. Baker CMOS Grade) at 55 °C for overnight to complete the transfer process. To decompose all PMMA, graphene sheets were annealed at 450 °C for 45 min under H_2/Ar atmospheres (20:80 sccm) at 500 Torr.

Graphene Device Fabrication: Four electrodes were made by applying silver paste at the corners of graphene sheets (5 mm × 5 mm) to form the device suitable for Hall effect measurements. And two of these electrodes were chosen as source and drain contacts for FET operation. To study the device in liquids, silicon rubber (Dow Corning 3140) was spread surrounding graphene to create a reservoir. The electrodes were also protected by rubber for insulation from electrolytes. A homemade holder was fabricated by connecting the samples with external circuits, as shown in Figure 1a.

Immobilization of DNA on Graphene: The single-strain sequence of probe, complementary, and one-base mismatched DNA (Sigma Aldrich) we used are presented below: probe) 5′-AGG-TCG-CCG-CCC-3′; complementary) 3′-TCC-AGC-GGC-GGG-5′; one-base mismatched) 3′-TCC-AGC-GGC-GTG-5′. The assigned concentrations of complementary and one-base mismatched DNA were prepared by diluting them with 1× PBS solution (UniRegion Bio-Tech). 1× PBS is composed of 13.7 mM NaCl, 0.27 mM KCl, 0.43 mM Na_2HPO_4, and 0.147 mM KH_2PO_4. Firstly the graphene device was incubated in 1× PBS for 2 h, and then 10 μM probe DNA was immobilized on it for 16 h at room temperature. A following rinsing step with DI water was carried out to remove weakly bound DNA. The complementary or one-base mismatched DNA were dropped onto the device in sequence from 10^{-3} nM to 10 nM for hybridization with probe DNA. It took 3 h for hybridization at each concentration and after that the rinsing step was always done. A full hybridization experiment was accomplished as a control study by mixing probe and complementary DNA in 1× PBS for several hours, and the mixture was then immobilized onto the device for 3 h, followed by a standard washing process. Moreover, the electrical signals were not reversible with DNA concentration because the complementary DNA exhibited strong interaction (through hydrogen bonding) with the probe DNA. The binding could not be broken simply by rinsing at room temperature. The detection experiment must be carried out by adding complementary DNA from low to high concentrations.

Electrical Measurements and Characterizations: The liquid-gated graphene FETs were measured in a semiconductor parameter analyzer (Keithley 4200-SCS). During measurement, a silver wire was used as a gate electrode. For the Hall effect measurement, the electrical properties of the samples were recorded by an NI PXI-1033 measurement unit. Raman spectra were collected in NT-MDT confocal Raman microscopic system (laser wavelength: 473 nm; laser power: 0.5 mW; spot size: ≈0.5 μm). The spectra taken from samples were calibrated against a Si peak at 520 cm^{-1}.

Supporting Information

Supporting Information is available from the Wiley Online Library or from the author.

Acknowledgements

C.-T.L. and P.T.K.L contributed equally to this work. This research was supported by National Science Council Taiwan (NSC-99-2112-M-001-021-MY3 and 99-2738-M-001-001) and Academia Sinica (IAMS and Nano program). The authors also acknowledge the support from NCTU Taiwan.

Received: September 15, 2012
Revised: October 24, 2012
Published online: January 9, 2013

[1] D. Li, S. P. Song, C. H. Fan, *Acc. Chem. Res.* **2010**, *43*, 631.
[2] J. Wang, *Electroanalysis* **2005**, *17*, 7.
[3] F. S. Lu, L. R. Gu, M. J. Meziani, X. Wang, P. G. Luo, L. M. Veca, L. Cao, Y. P. Sun, *Adv. Mater.* **2009**, *21*, 139.
[4] D. L. Fu, H. L. Lim, Y. M. Shi, X. C. Dong, S. G. Mhaisalkar, Y. Chen, S. Moochhala, L. J. Li, *J. Phys. Chem. C* **2008**, *112*, 650.
[5] Y. X. Huang, H. G. Sudibya, D. L. Fu, R. H. Xue, X. C. Dong, L. J. Li, P. Chen, *Biosens. Bioelectron.* **2009**, *24*, 2716.

[6] X. W. Tang, S. Bansaruntip, N. Nakayama, E. Yenilmez, Y. L. Chang, Q. Wang, *Nano Lett.* **2006**, *6*, 1632.
[7] E. L. Gui, L. J. Li, P. S. Lee, A. Lohani, S. G. Mhaisalkar, Q. Cao, S. J. Kang, J. A. Rogers, N. C. Tansil, Z. Q. Gao, *Appl. Phys. Lett.* **2006**, *89*, 232104.
[8] E. L. Gui, L. J. Li, K. K. Zhang, Y. P. Xu, X. C. Dong, X. N. Ho, P. S. Lee, J. Kasim, Z. X. Shen, J. A. Rogers, S. G. Mhaisalkar, *J. Am. Chem. Soc.* **2007**, *129*, 14427.
[9] K. Maehashi, T. Katsura, K. Kerman, Y. Takamura, K. Matsumoto, E. Tamiya, *Anal. Chem.* **2007**, *79*, 782.
[10] S. Sorgenfrei, C. Y. Chiu, R. L. Gonzalez, Y. J. Yu, P. Kim, C. Nuckolls, K. L. Shepard, *Nat. Nanotechnol.* **2011**, *6*, 125.
[11] A. K. Geim, K. S. Novoselov, *Nat. Mater.* **2007**, *6*, 183.
[12] Y. M. Lin, P. Avouris, *Nano Lett.* **2008**, *8*, 2119.
[13] G. Eda, G. Fanchini, M. Chhowalla, *Nat. Nanotechnol.* **2008**, *3*, 270.
[14] L. J. Cote, F. Kim, J. X. Huang, *J. Am. Chem. Soc.* **2009**, *131*, 1043.
[15] C. Y. Su, Y. P. Xu, W. J. Zhang, J. W. Zhao, X. H. Tang, C. H. Tsai, L. J. Li, *Chem. Mater.* **2009**, *21*, 5674.
[16] Z. Y. Yin, S. Y. Sun, T. Salim, S. X. Wu, X. A. Huang, Q. Y. He, Y. M. Lam, H. Zhang, *ACS Nano* **2010**, *4*, 5263.
[17] Y. X. Liu, X. C. Dong, P. Chen, *Chem. Soc. Rev.* **2012**, *41*, 2283.
[18] J. T. Robinson, F. K. Perkins, E. S. Snow, Z. Q. Wei, P. E. Sheehan, *Nano Lett.* **2008**, *8*, 3137.
[19] J. D. Fowler, M. J. Allen, V. C. Tung, Y. Yang, R. B. Kaner, B. H. Weiller, *ACS Nano* **2009**, *3*, 301.
[20] V. Dua, S. P. Surwade, S. Ammu, S. R. Agnihotra, S. Jain, K. E. Roberts, S. Park, R. S. Ruoff, S. K. Manohar, *Angew. Chem. Int. Ed.* **2010**, *49*, 2154.
[21] Y. Lu, B. R. Goldsmith, N. J. Kybert, A. T. C. Johnson, *Appl. Phys. Lett.* **2010**, *97*, 083107.
[22] Y. Ohno, K. Maehashi, Y. Yamashiro, K. Matsumoto, *Nano Lett.* **2009**, *9*, 3318.
[23] C. H. Lu, H. H. Yang, C. L. Zhu, X. Chen, G. N. Chen, *Angew. Chem. Int. Ed.* **2009**, *48*, 4785.
[24] A. Bonanni, M. Pumera, *ACS Nano* **2011**, *5*, 2356.
[25] Z. Y. Yin, Q. Y. He, X. Huang, J. Zhang, S. X. Wu, P. Chen, G. Lu, Q. C. Zhang, Q. Y. Yan, H. Zhang, *Nanoscale* **2012**, *4*, 293.
[26] Q. Y. He, H. G. Sudibya, Z. Y. Yin, S. X. Wu, H. Li, F. Boey, W. Huang, P. Chen, H. Zhang, *ACS Nano* **2010**, *4*, 3201.
[27] N. Mohanty, V. Berry, *Nano Lett.* **2008**, *8*, 4469.
[28] Y. Ohno, K. Maehashi, K. Inoue, K. Matsumoto, *Jpn. J. Appl. Phys.* **2011**, *50*, 070120.
[29] K. S. Kim, Y. Zhao, H. Jang, S. Y. Lee, J. M. Kim, J. H. Ahn, P. Kim, J. Y. Choi, B. H. Hong, *Nature* **2009**, *457*, 706.
[30] A. Reina, X. T. Jia, J. Ho, D. Nezich, H. B. Son, V. Bulovic, M. S. Dresselhaus, J. Kong, *Nano Lett.* **2009**, *9*, 30.
[31] C. Y. Su, A. Y. Lu, C. Y. Wu, Y. T. Li, K. K. Liu, W. J. Zhang, S. Y. Lin, Z. Y. Juang, Y. L. Zhong, F. R. Chen, L. J. Li, *Nano Lett.* **2011**, *11*, 3612.
[32] X. C. Dong, Y. M. Shi, W. Huang, P. Chen, L. J. Li, *Adv. Mater.* **2010**, *22*, 1649.
[33] Y. X. Huang, X. C. Dong, Y. M. Shi, C. M. Li, L. J. Li, P. Chen, *Nanoscale* **2010**, *2*, 1485.
[34] J. A. Lin, D. Teweldebrhan, K. Ashraf, G. X. Liu, X. Y. Jing, Z. Yan, R. Li, M. Ozkan, R. K. Lake, A. A. Balandin, C. S. Ozkan, *Small* **2010**, *6*, 1150.
[35] a) M. Dankerl, M. V. Hauf, A. Lippert, L. H. Hess, S. Birner, I. D. Sharp, A. Mahmood, P. Mallet, J. Y. Veuillen, M. Stutzmann, J. A. Garrido, *Adv. Funct. Mater.* **2010**, *20*, 3117; b) X. S. Li, W. W. Cai, J. H. An, S. Kim, J. Nah, D. X. Yang, R. Piner, A. Velamakanni, I. Jung, E. Tutuc, S. K. Banerjee, L. Colombo, R. S. Ruoff, *Science* **2009**, *324*, 1312.
[36] X. S. Li, W. W. Cai, J. H. An, S. Kim, J. Nah, D. X. Yang, R. Piner, A. Velamakanni, I. Jung, E. Tutuc, S. K. Banerjee, L. Colombo, R. S. Ruoff, *Science* **2009**, *324*, 1312.
[37] C. Y. Su, D. L. Fu, A. Y. Lu, K. K. Liu, Y. P. Xu, Z. Y. Juang, L. J. Li, *Nanotechnology* **2011**, *22*, 185309.
[38] A. Star, E. Tu, J. Niemann, J. C. P. Gabriel, C. S. Joiner, C. Valcke, *Proc. Natl. Acad. Sci. USA* **2006**, *103*, 921.
[39] X. C. Dong, D. L. Fu, Y. P. Xu, J. Q. Wei, Y. M. Shi, P. Chen, L. J. Li, *J. Phys. Chem. C* **2008**, *112*, 9891.
[40] N. Varghese, U. Mogera, A. Govindaraj, A. Das, P. K. Maiti, A. K. Sood, C. N. R. Rao, *ChemPhysChem* **2009**, *10*, 206.
[41] D. O. Jordan, in *The Nucleic Acids* (Eds: E. Chargaff, J. N. Davidson), Academic Press, New York **1955**.
[42] H. M. Nie, S. T. Khew, L. Y. Lee, K. L. Poh, Y. W. Tong, C. H. Wang, *J. Controlled Release* **2009**, *138*, 64.
[43] E. Dubuisson, Z. Y. Yang, K. P. Loh, *Anal. Chem.* **2011**, *83*, 2452.
[44] W. R. Yang, K. R. Ratinac, S. P. Ringer, P. Thordarson, J. J. Gooding, F. Braet, *Angew. Chem. Int. Ed.* **2010**, *49*, 2114.
[45] Q. Y. He, S. X. Wu, Z. Y. Yin, H. Zhang, *Chem. Sci.* **2012**, *3*, 1764.
[46] S. Liu, X. F. Guo, *NPG Asia Mater.* **2012**, *4*, e23.
[47] T.-Y. Chen, P. T. K. Loan, C.-L. Hsu, Y.-H. Lee, J. Tse-Wei Wang, K.-H. Wei, C.-T. Lin, L.-J. Li, *Biosens. Bioelectron.* **2012**, DOI: 10.1016/j.bios.2012.07.059.